Submitted for publication to *Phys. Rev. Lett.*

The Microscopic and Macroscopic Structure of the Precursor Layer in Spreading Viscous Drops

H. Pirouz Kavehpour[a)], Ben Ovryn[b)], Gareth H. McKinley[a)]

[a)]Hatsopoulos Microfluids Laboratory, Department of Mechanical Engineering, Massachusetts Institute of Technology, Cambridge, MA. [b)]Department of Biomedical Engineering, Case Western Reserve University, Cleveland, OH.

October 18, 2002

We study the spreading of viscous non-volatile liquids on smooth horizontal substrates using a phase-modulated interference microscope with sufficient dynamic range to enable the simultaneous measurement of both the inner ('microscopic') length scale and the outer ('macroscopic') flow scale in addition to the intermediate matching region. The resulting measurements of both the apparent contact angle and the lateral scale of the precursor 'wetting' film agree quantitatively with theoretical predictions for a van der Waal's liquid over a wide range of capillary numbers.

PAC numbers: 6810Gw, 6125Hq,6810Cr, 6845Gd

When a completely wetting liquid spreads sufficiently slowly on a clean smooth substrate, a very thin precursor film may propagate ahead of what the naked eye, or the eye aided by conventional microscopes, perceives to be the apparent or macroscopic wetting line. Hardy's pioneering experimental work[1] provided the first evidence of the existence of a very thin liquid film in front of a spreading front on solid surfaces. Numerous studies have subsequently confirmed the existence of precursor films using ellipsometry[2,3], interference patterns[3], and polarized reflection microscopy[4]. The available experimental results, have demonstrated qualitatively the existence of the precursor film[4] but there has not been an adequate comparison of the results with the theory[2].

A simplifying feature of wetting via a precursor film is that flow within the film is virtually one-dimensional and can be described by a lubrication analysis. More significantly, the spreading of the bulk liquid is effectively decoupled from the motion of the wetting line, and is independent of the spreading coefficient, *S*. This has been well-documented both experimentally and theoretically[4,5]. The liquid may be considered to spread across a thin film of a pre-wetted surface; however the thickness of this precursor layer remains indeterminate. Under these conditions, the hydrodynamic equations can be solved explicitly, and the velocity dependence of the macroscopically-observable apparent contact angle is predicted to follow a simple cubic power-law[5,6] known commonly as Tanner's law or more correctly as the Hoffman-Voinov-Tanner relationship[7] with $\theta_a \sim Ca^{1/3}$ where θ_a is the apparent dynamic contact angle and $Ca=\mu U/\sigma$ is the capillary number. Here μ and σ are the (constant) viscosity and surface tension of the Newtonian liquid and U is the spreading velocity of the drop.

Theoretical analysis of dynamic wetting in the precursor layer ahead of the macroscopic droplet has focused primarily on nonvolatile liquid drops spreading on smooth surfaces. The analysis assumes that long range fluid/solid interactions are the only driving forces for the precursor film, and that the film remains thick enough so that the continuum theory remains valid. In this case, the sum of fluid/solid interactions as a function of the film thickness, $h(x)$, can be lumped into the disjoining pressure[8], $\Pi_{\mathrm{vdW}} = A/6\pi h^3$ where A is the effective Hamaker constant. In the lubrication analysis of thin liquid films, this disjoining pressure gives rise to a pressure gradient that competes with the capillary pressure and viscous resistance to flow[9].

Theoretical studies by Hervet & de Gennes[5,9], show that, in contrast to the 'outer region', the inner dynamics do depend on the spreading coefficient, *S*. At short times, when the precursor layer is advancing 'adiabatically'[10], the length of the 'adiabatic' precursor layer, L_P, is predicted to be inversely proportional to the spreading velocity (or the capillary number) of the film at a given time after the start of spreading;

$$L_P = \ell_{micro}\sqrt{\frac{S}{\sigma}}\,\frac{\sigma}{\mu U} = \sqrt{\frac{SA}{6\pi\sigma^2}}\,\frac{1}{Ca} \qquad (1)$$

where $\ell_{micro} \equiv \sqrt{A/6\pi\sigma}$ is a molecular length scale.

The solution to the governing equation[5,9] has the property that $h(x)$ has an inflection point (at a point denoted $h_i(x_i)$) corresponding to the intersection with the precursor film as indicated in Fig. 1. The existence of this inflection point is a requirement for drops with small apparent contact angles and provides a connection between the inner 'microscopic' region near the 'tongue' and the outer macroscopic region. The location of this inflection point can vary with the spreading velocity of the drop and has seldom been quantified. The matching region is commonly treated theoretically as a viscous flow in a wedge[5,11] however, very careful recent simulations[12] show that the matching requirement in fact strongly couples the inner and outer solutions and affects the constant of proportionality that appears in Tanner's law.

The disparate range of length scales between the inner and outer structure of the drop profile

complicate experimental studies of this matching problem, because a method with large dynamic range is required to simultaneously probe each region. Auserré and co-workers[4] confirmed the macroscopic form of Tanner's law and simultaneously demonstrated the existence of a 'diffusive' precursor film using ellipsometric contrast. However, due to the limitation in instrument range ($h \leq$ 400 Å), the transition from the 'diffusive' precursor layer to the intermediate and macroscopic regions were not investigated[13]. An early microscopic study by Beaglehole[2] supported the dependence of L_P on velocity qualitatively but the results do not span a wide range of capillary number and it is difficult to separately assess the effects of viscosity and surface tension.

Because experiments have not yet been performed which simultaneously confirm the existence of the macroscopic and microscopic descriptions of the spreading process and quantitatively interconnect the two processes, we have measured the length of precursor films using a novel interference microscope with both high temporal and spatial dynamic range. We have combined an electro-optically phase-shifting laser feedback interferometer (LFI) together with a reflecting light microscope[14]. The resulting interference microscope was used to measure the variation of the optical path length and fringe visibility (which is proportional to the sample reflectivity) in the vicinity of an advancing wetting line. Light from a low power helium-neon laser was passed through a linear polarizer and electro-optic phase modulator (New Focus, 4002) and focused with a 20×/0.4 NA objective lens (Zeiss, Epiplan). After reflection from the surface of interest, the light re-enters the laser cavity. The time-dependent change in the laser intensity was measured with a detector (New Focus, 1801) that monitored the light transmitted through the rear mirror of the laser. Calibration tests indicate that the lateral spatial resolution of this system is approximately 0.8 μm and that the optical path length may be measured with an rms error of about 10 nm, with a response time of ~ 2 ms.

We have used the same experimental geometry as earlier investigations[2,4,15] and consider well-characterized silicone oils spreading on polished silicon wafers. First, we deposit a drop of silicone oil of a known volume on a cleaned silicon wafer using a syringe pump (Harvard Apparatus, pump 11). When the advancing contact line of the spontaneously wetting drop moves below the focal point of the objective lens its instantaneous rate of spreading, $\dot{R}$, is measured using a CCD camera and the profile, $h(t)$, is measured interferometrically. Knowing the local speed of the wetting line, the profile of the drop, $h(t)$, is converted to $h(x)$ via a simple Gallilean transformation.

The spreading velocity $U=\dot{R}(t)$ of the drop is a time-varying function that depends on the drop size and the dominant driving and resisting forces[16]. The drops used in the present experiments have a volume V = 10μL and initially assume the shape of a spherical cap (which spreads such that $R \sim t^{1/10}$) but ultimately evolve to a 'pancake' regime ($R \sim t^{1/7}$)[16,17]. All of our measurements are performed when the drops are in the final pancake regime.

A number of different silicone fluids have been used in our experiments in order to generate results for a wide range of capillary numbers. These materials are supplied by Gelest Inc. and have constant shear viscosities spanning the range $7\times10^{-3} \leq \mu \leq 10.0$ Pa.s. The surface tension, σ, of these silicone liquids vary weakly with increasing molecular weight but are in the range of 19×10^{-3} - 21×10^{-3}N/m. Further details of the rheological properties are provided elsewhere[16].

A representative drop profile is presented in Fig. 2, where the abscissa represents the lateral displacement (x) of the front and the left ordinate shows the measured value of the decrease in optical path length (or local thickness of the drop, $h(x)$) in μm. To convert the measured phase to drop height, we used n=1.4 for the index of refraction of the liquid. The solid line represents the interferometric fringe visibility, m, and is represented on the right ordinate axis. The fringe visibility, m, remains constant until the edge of the precursor film reaches the focal point of the laser interferometer. At this instant, the fringe visibility decreases rapidly, well in advance of the macroscopic front reaching the measurement point. The inset to Fig. 2 shows that a thin liquid precursor film or 'tongue' of fluctuating but approximately constant thickness H_p = 99 ± 10 nm preceding the macroscopic contact line is the cause of the drop in the fringe visibility. This decrease in fringe visibility is the interferometric equivalent of the impeded condensation of humid air that can be observed using a 'breath test'[3]. Later in the spreading process, the macroscopic front passes through the measuring volume and the macroscopic profile of the drop can be accurately imaged. Rather than assuming a model–dependent drop profile, the local slope was determined by a direct numerical differentiation of the profile $h(x)$ using a fifth order Gram polynomial[18] that minimizes amplification of experimental noise. As shown in Fig. 3(a), at $Ca=7\times10^{-4}$, the slope dh/dx has a maximum value at a distance of 13 μm from the point that the macroscopic profile of the

drop and the precursor layer meet, corresponding to an inflection point of the drop profile. By definition[12,19], this point separates the inner region of 'microscopic physics' from the 'outer' or macroscopic domain. The macroscopic dynamic contact angle is conventionally defined[19] as $\max\left\{\tan^{-1}\left(dh/dx\right)\right\}$ and we can thus determine unambiguously a precise value for θ_a. As the spreading proceeds, the capillary number falls and the maximum slope or apparent contact angle decreases[4] as $\theta_a \sim t^{-0.3}$.

In Fig. 3(b), we show the variation in the measured dynamic contact angle θ_a (in radians) as a function of the capillary number for $2\times10^{-6} \le Ca \le 3.2\times10^{-4}$. Numerous functional forms for the variation in with *Ca* have been proposed in the literature and can be compared impartially with this data. Direct regression to the familiar and oft-quoted Tanner's law ($\theta_a = k_1 Ca^{1/3}$) gives $k_1 = 1.92 \pm 0.04$ with a confidence level of $R^2=0.968$ and is shown by the broken line. Careful examination shows that in fact there is a systematic deviation from this line. A better fit to the data set is given by a somewhat stronger power-law, $\theta_a = k_2 Ca^n$ with $k_2 = 3.4 \pm 0.4$ and $n = 0.39 \pm 0.01$ (at a confidence level of $R^2 = 0.986$). Previous experiments have also noted a power law exponent exceeding $n = 1/3$[6,15]. However, as noted first by de Gennes, there is in fact a weak logarithmic dependency of the numerical coefficient k_1 on the speed of the spreading drop. A more detailed treatment[20] gives an equation of the functional form $\theta_a = k_3\left(Ca\ln\left(k_4 Ca^{2/3}\right)\right)^{1/3}$ with $k_4 \sim \ell_{macro}/\ell_{micro}$. Here ℓ_{macro} is a characteristic matching length where the inner 'microscopic' profile matches the outer macroscopic profile of the drop. Regression to this form is shown by the solid line in Fig. 3(b) and yields $k_3 = 1.2 \pm 0.7$ and $k_4 = 32450 \pm 23276$ with a confidence level of $R^2 = 0.987$. It therefore appears that this logarithmic dependence is the correct functional form to be used as a correction to Tanner's law which becomes increasingly important at small *Ca*. A recent computation[20] suggests that $k_4 = 1.44\ell_{micro}/\ell_{macro}$ as the matching length can be calculated by substituting experimental values of ℓ_{micro} (see below) and k_4 in this relation. We find $\ell_{macro} \cong 14\mu m$ which, according to our measurements, is the average distance from the inflection point to the intersection of the macroscopic region and the precursor layer for the range of capillary numbers in our experiments. This length scale is large with respect to the microscopic region (ℓ_{micro}) but still small with respect to outer scales such as the capillary length $\ell_{cap} = \left(\sigma/\rho g\right)^{1/2} = 1.4\,\text{mm}$ or the Landua-Levich-Deryagiun length $\ell_{LLD} \approx \ell_{cap} Ca^{1/3}$ which is important in forced wetting[20].

In original asymptotic theories[5,20] the front factor in the spreading law is determined from the wedge flow in the intermediate matching region to be $k_3 = 9^{1/3} \cong 2.08$. Our experiments yield a smaller value that is consistent with earlier experiments in the same system[4]. This so-called 'size effect'[7,21] arises from two distinct physical phenomena; (i) the additional curvature resulting from the geometry of the spherical caps formed by the very small fluid droplets and (ii) the coupling between the inner and outer scales. We have performed additional experiments (not shown here) using two-dimensional silicon strips that yield a somewhat larger front factor, k_3' = 1.7). The latter effect was demonstrated by recent simulations[12] which show that the front factor varies systematically with the 'van der Waals' number $G = (\ell_{micro}/\ell_{cap})^2$. For the present silicone/silicon system $G \approx 1.8\times10^{-13}$.

We have also determined the length of the 'adiabatic' precursor film, L_P, for the spontaneously spreading liquid drops for a wide range of capillary numbers. It is important to note that the 'diffusive' precursor films[10] which usually develop at longer times are not part of this analysis. We define L_P as the distance from the point that the fringe visibility, m, suddenly decreases from the constant value corresponding to the bare silicon wafer surface to the point that the macroscopic profile is measured (inset of Fig. 2). In Fig. 4, we show the length of the precursor film L_P, as a function of capillary number, *Ca*. The length of the precursor film decreases monotonically as the spreading rate of the drop or fluid viscosity increases. Regression to a power-law relationship yields a best fit, $L_P = 7.2\times10^{-10} Ca^{-0.98\pm0.16}$ with L_P in meters. This result is in excellent agreement with the form of the theoretical prediction[5,9] in equation (1). Furthermore, the front factor is in good agreement with the calculated value of $\sqrt{SA/6\pi\sigma^2} \cong 6.1\times10^{-10}\,\text{m}$ (using available literature values of $S \cong 20\times10^{-3}$ N/m, $A = 1.4\times10^{-19}$ J)[4,15,22] which is shown by the dashed line in Fig. 4. The inset of Fig. 4 shows the average thickness of the adiabatic precursor film, H_P (in nm), as a function of capillary number. As can be seen from Fig. 2, significant local fluctuations in this local measurement of the precursor film can be measured using the psLFI technique; however there is no evidence of a dependency of the average thickness H_P on

capillary number and a constant average thickness of 98 ± 20 nm is measured.

To summarize, we have applied a non-invasive phase-shifting laser feedback interference microscope to investigate the evolution of the precursor films ahead of moving contact lines in 'dry spreading' of perfectly wetting van der Waals fluids. The system has sufficient resolution and dynamic range to resolve details of both the physics of the inner (microscopic) interfacial region and its interconnection to the outer (macroscopic) fluid response. The coupling between these regimes that is revealed by the experimental measurements is in good agreement with theoretical predictions and numerical simulation. The variation in apparent contact angle with *Ca* is roughly consistent with the Hoffman-Tanner-Voinov relationship; however careful examination shows the clear existence of a logarithmic dependence on the spreading velocity or capillary number as predicted previously by de Gennes. Furthermore, we have shown that the length of the 'adiabatic' precursor film, L_P, that forms in advance of the drop during the early stages of spreading is inversely proportional to the capillary number as anticipated theoretically.

This research was supported by the NASA Microgravity fluid physics program under grant NAG3-2155. The authors would like to acknowledge stimulating discussions with S. Garoff, S. H. Davis, H. A. Stone and J. Eggers on the topic of moving contact lines.

[1] W.P. Hardy, Philos. Mag. **38**, 49 (1919).
[2] D. Beaglehole, J. Phys. Chem. **93**, 893 (1989).
[3] W.D. Bascom, R.L. Cottington, and C.R. Singleterry, in *Contact angle, wettability, and adhesion*, edited by F.M. Fowkes (ACS, Washington, DC, 1964), Vol. 43, pp. 355.
[4] D. Ausserré, A.M. Picard, and L. Léger, Phys. Rev. Lett. **57** (21), 2671 (1986).
[5] P.-G. de Gennes, Rev. Mod. Phys. **57**, 827 (1985).
[6] L. H. Tanner, J. Phys. D: Appl. Phys. **12**, 1473 (1979).
[7] S.F. Kistler, in *Wettability*, edited by J.C. Berg (Marcel Dekker Inc., New York, 1993), Vol. 49, pp. 311.
[8] B.V. Derjaguin, Colloid J. USSR (English translation) **10**, 25 (1955).
[9] H. Hervet and P.-G. de Gennes, C. R. Acad. Sci. Paris **299** (II), 499 (1984).
[10] J.P. Joanny and P.-G. de Gennes, J. Phys. **47** (1), 121 (1986).
[11] L.M. Hocking and A.D. Rivers, J. Fluid Mech. **121**, 425 (1982).
[12] L.M. Pismen, B.Y. Rubinstein, and I. Bazhlekov, Phys. Fluids **12** (3), 480 (2000).
[13] L. Leger, M. Erman, A.M. Guinet-Picard, D. Ausserré, and C. Strazielle, Phys. Rev. Lett. **60** (23), 2390 (1988).
[14] B. Ovryn and J.H. Andrews, Opt. Lett. **23** (14), 1078 (1998).
[15] J.-D Chen and N. Wada, J. Coll. Inter. Sc. **148** (1), 207 (1992).
[16] H.P. Kavehpour, B. Ovryn, and G.H. McKinley, Coll. Surf. A. **206**, 409 (2002).
[17] A. Oron, S.H. Davis, and S.G. Bankoff, Rev. Mod. Phys. **69** (3), 931 (1997).
[18] S. Whitaker and R.L. Pigford, Ind. Eng. Chem. **52** (2), 185 (1960).
[19] S. Middleman, *Modeling axisymmetric flows*. (Acadenic Press, Inc., San Diego, Ca, 1995).
[20] J. Eggers and H.A. Stone, Preprint.
[21] E.B. Dussan V, Ann. Rev. Fluid Mech. **11**, 371 (1979).
[22] P. Hiemenz and R. Rajagopalan, *Principles of Colloid and Surface Chemistry*. (Marcel Dekker, New York, 1997).

List of Figures:

FIG. 1: Schematic of macroscopic and microscopic features in the vicinity of an advancing contact line of a perfectly wetting van der Waals fluid spreading slowly over a smooth dry substrate.

FIG. 2: Evolution in the profile of a silicone oil drop spreading on a smooth dry silicon substrate at $Ca=2\times10^{-6}$. Symbols (○) show the local thickness of the drop (in μm) and solid line (——) is the visibility of the interference fringes, m. The inset shows an enlarged view of the precursor film detected in front of the moving contact line. Each symbol is drawn to the scale of the lateral resolution of the psLFI system ($\Delta x \sim \pm 0.6$ μm).

FIG. 3: (a) Drop profile, $h(x)$, and the spatial derivative, dh/dx for different values of capillary number ($Ca= 1\times10^{-4}$ and $Ca = 7\times10^{-4}$). The maximum value of the slope corresponds to the macroscopic dynamic contact angle, θ_a. (b) Dynamic contact angle, θ_a, as a function of capillary number. Dashed line (– – –) is the regression to the experimental data following Tanner's law, $\theta_a = k_1 Ca^{1/3}$. Dashed dot line (— - —) is a regression to the experimental data of form, $\theta_a = k_2 Ca^{n}$. The solid line (——) is a regression to the experimental data using de Gennes model, $\theta_a = k_3\left(Ca\ln\left(k_4 Ca^{2/3}\right)\right)^{1/3}$. The inset shows de Gennes model fit to the same set of data (solid line) when the reduced angle θ_a^3 / Ca is plotted as a function of $\ln(Ca)$. The slope of the solid line is 1/3.

FIG. 4: Length of the precursor film, L_P, (in meters) as a function of capillary number. Solid line (——) is the regression to the experimental results (●), $L_P = 7.2\times10^{-10} Ca^{-0.98\pm0.16}$, and the dashed line (– – –) is the theoretical prediction for an 'adiabatic' precursor layer, $L_P = 6.1\times10^{-10} Ca^{-1}$. The dash-dot line (— - —) is the diffraction limited lateral resolution of our system. The inset shows the average thickness of the precursor film, H_P, as a function of capillary number, Ca.

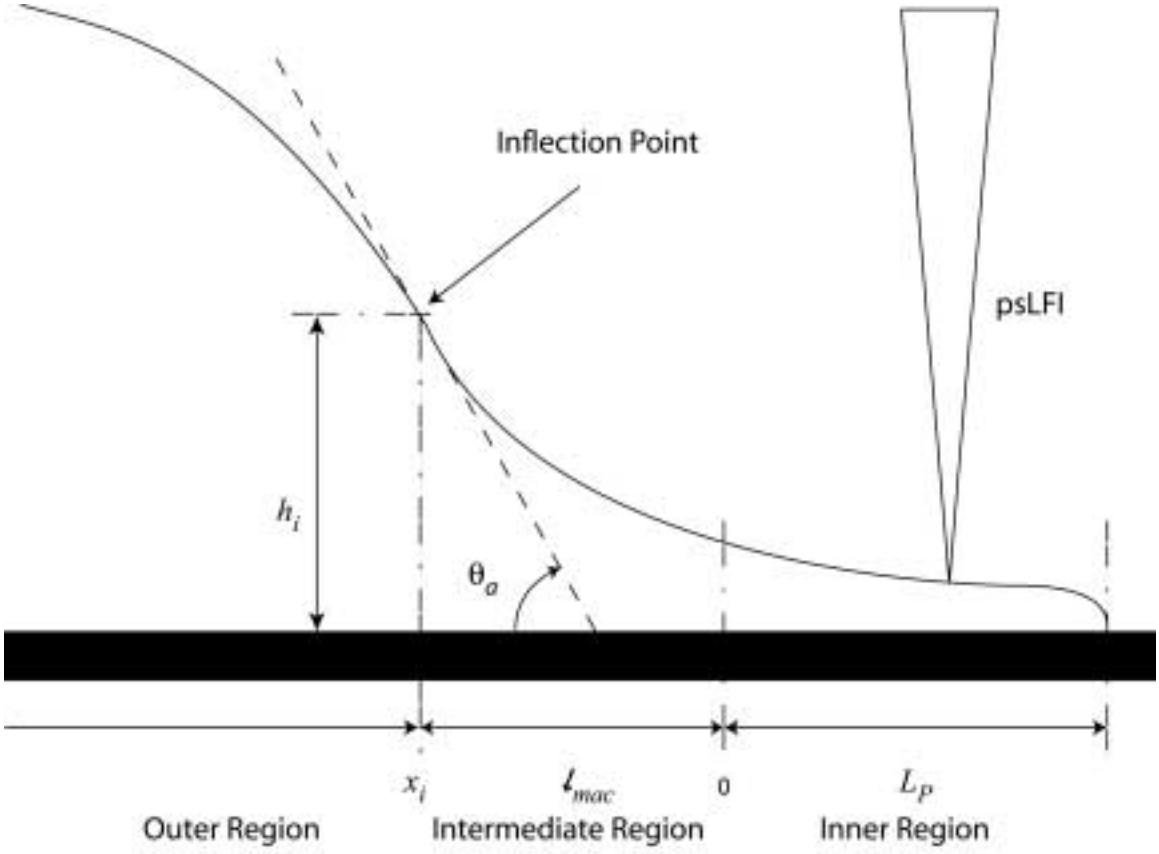

FIG. 1, Kavehpour et al, *Phys. Rev. Lett.*

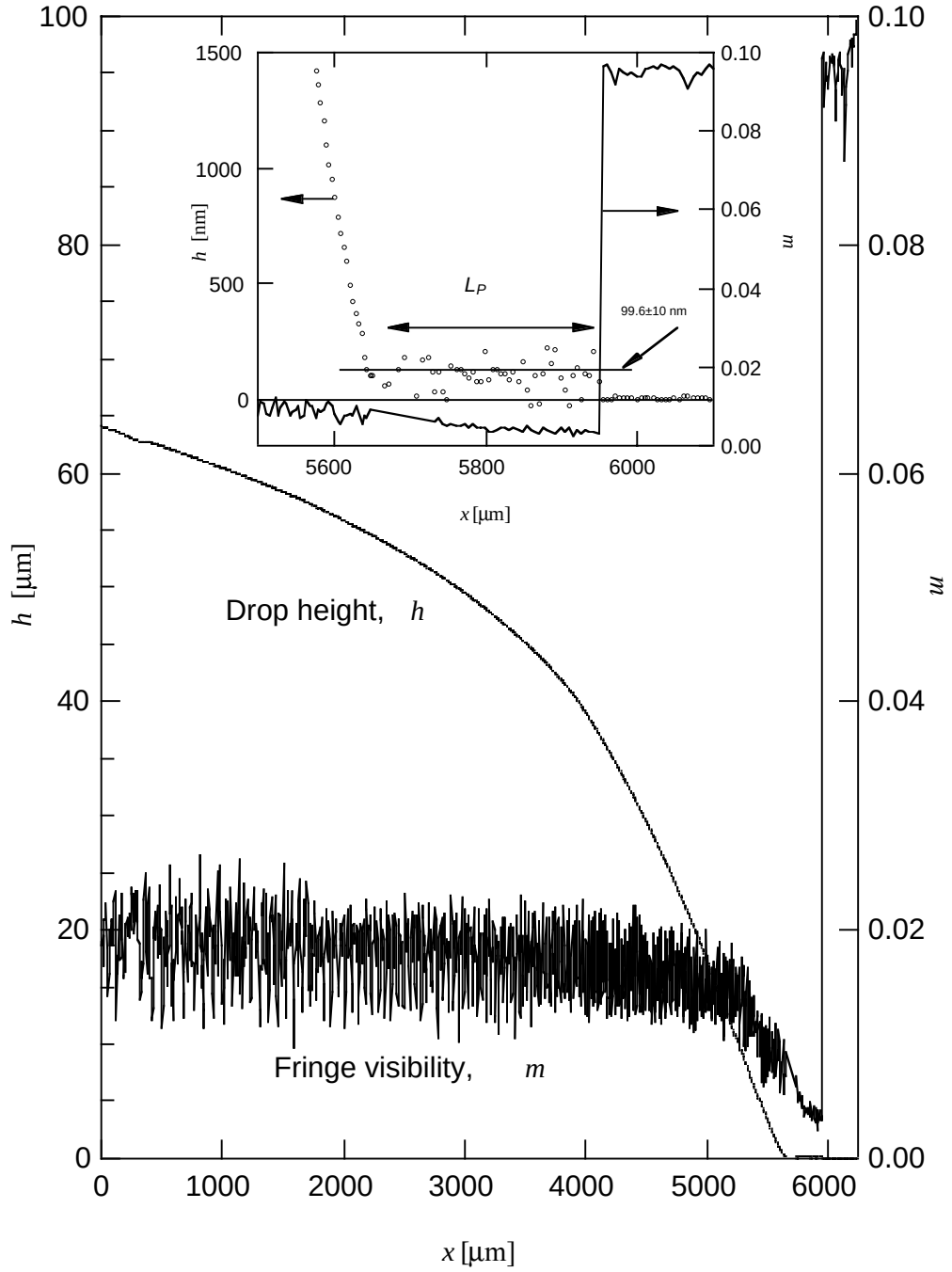

FIG. 2, Kavehpour et al, *Phys. Rev. Lett.*

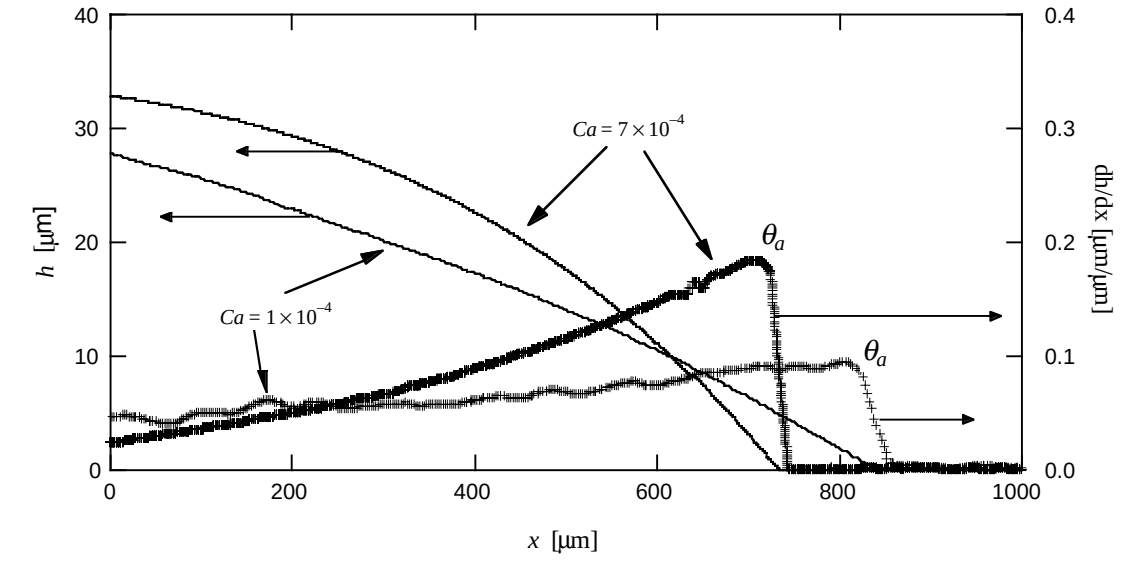

(a)

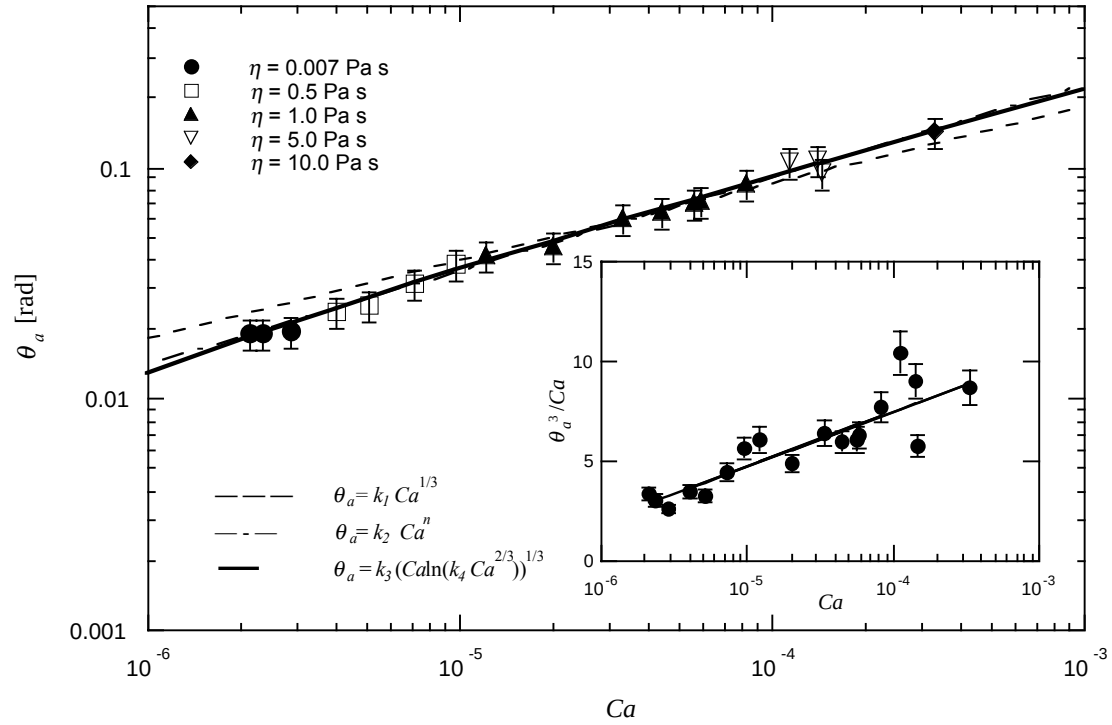

(b)

FIG. 3, Kavehpour et al, *Phys. Rev. Lett.*

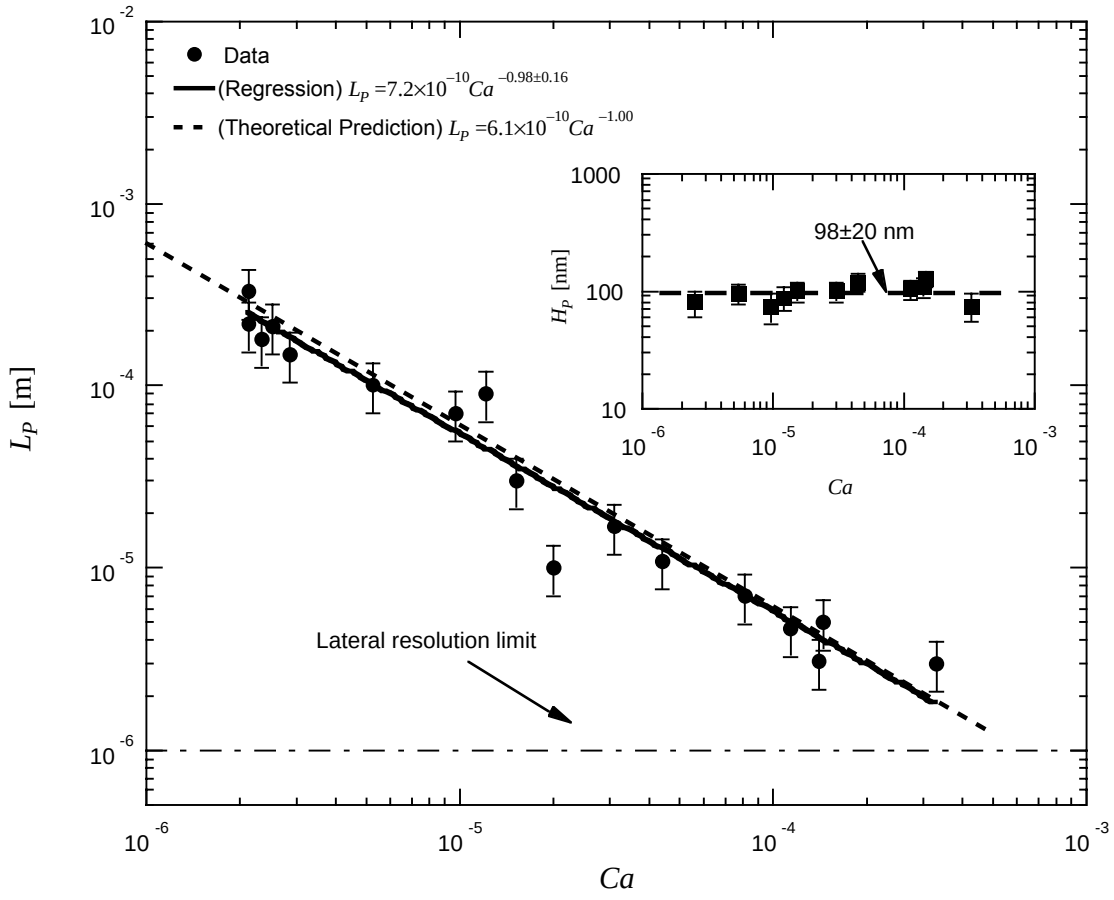

FIG. 4, Kavehpour et al, *Phys. Rev. Lett.*